International Journal of Nanomedicine

Dovepress
open access to scientific and medical research

Open Access Full Text Article

ORIGINAL RESEARCH

Optimum Preparation Method for Self-Assembled PEGylation Nano-Adjuvant Based on *Rehmannia glutinosa Polysaccharide* and Its Immunological Effect on Macrophages

This article was published in the following Dove Press journal:
International Journal of Nanomedicine

Yee Huang[1]
Li Nan[1,2]
Chenwen Xiao[1]
Quanan Ji[1]
Ke Li[1]
Qiang Wei[1]
Yan Liu[1]
Guolian Bao[1]

[1]Institute of Animal Husbandry and Veterinary Medicine, Zhejiang Academy of Agricultural Science, Hangzhou 310021, People's Republic of China; [2]Zhejiang Normal University, Jinhua 321000, People's Republic of China

Background: *Rehmannia glutinosa* polysaccharide is the main reason that contributes to the immunological function of *R. glutinosa*. Due to its disadvantages in clinical use, here we designed the PEGylation nano-RGP (pRL) to improve the drug-targeting effect and the immunological function. Our present work aims to establish the optimum condition of preparing the pRL and to investigate its immunological function on macrophages.

Methods: pRL was prepared by thin film hydration method combined with ultra-sonication technique. And its preparation conditions were optimized with response surface methodology. Also, the lyophilization method was optimized. The characteristics of the pRL were evaluated, including particle size, drug loading, encapsulation efficiency and morphology. The immunological function of pRL on macrophage was investigated through CCK-8 test, ELISA and flow cytometry.

Results: The lipid-to-cholesterol molar ratio of 8:1, the addition of DSPE-PEG_{2000} of 9% and the lipid-to-drug ratio of 5.4:1 were the optimum preparation technology for pRL. The encapsulation efficiency (EE) of pRL under this preparation technology was 95.81±1.58%, with a particle size of 31.98 ± 2.6 nm. The lactose-to-lipid ratio (2:1) was the optimal lyophilization method. pRL promoted macrophage proliferation, which is significantly better than that of nano-RGP without PEGylation (RL). pRL-stimulated RAW264.7 cells showed a high secretion of pro-inflammatory cytokines, which is the characteristic indicator of M1 polarization. Enhanced cellular uptake through macropinocytosis-dependent and caveolae-mediated endocytosis was observed in pRL-treated RAW264.7 cells.

Conclusion: Our study concluded that PEGylation effectively overcame the poor targeting effect of *Rehmannia glutinosa* polysaccharide (RGP) and significantly improved the immunological profile of its nano-formulation, which suggested that pRL could serve as an immune adjuvant in clinical application.

Keywords: *Rehmannia glutinosa* polysaccharide, PEGylation, preparation technology, lyophilization method, macrophages

Correspondence: Yan Liu; Guolian Bao
Institute of Animal Husbandry and Veterinary Medicine, Zhejiang Academy of Agricultural Science, Hangzhou 310021, People's Republic of China
Email 35792191@qq.com; baoguolian@163.com

Introduction

Basic immunology has taken great strides in recent decades, and many underlying mechanisms of immune activation and tolerance have been discovered. This depth of knowledge has begun to give rise to the burgeoning field of immunomodulatory biomaterials,[1] among which self-assembled materials represent a unique opportunity

submit your manuscript | www.dovepress.com
DovePress
http://doi.org/10.2147/IJN.S221398

to generate well-controlled nanoparticles from a diverse range of molecular building blocks, such as lipids, synthetic polymers and peptides.[2,3] Taking advantage of nanoparticles' immunomodulatory properties, various nano-adjuvants have been researched and developed, but the translation from bench studies to clinical use has seen relatively little success. This has sparked an intense interest in the rational design and the preparation method optimization of nano-adjuvant that provide well-characterized mechanisms of action to trigger immune responses.

Lipid-based nano-vehicles are attractive for drug delivery applications for numerous reasons, including their resemblance to cell membranes in both structure and composition. They tend to be slightly sterically unstable and are cleared rapidly from the bloodstream. When contemplating the question of drug delivery, modification of the nano-carrier must be considered in order to keep it in circulation for the longest possible time to ensure target accumulation.

Polyethylene glycol (PEG), a non-toxic, non-immunogenic polymer, is widely utilized in drug delivery and nanotechnology due to its reported "stealth" properties and biocompatibility. PEGylation changes the physical and chemical properties of the nano-carriers, such as its conformation, electrostatic binding and hydrophobicity, and results in an improvement in the pharmacokinetic profile of the nanoparticles. It could improve the particle stability, enhance the targeting effect, prolong circulation time and reduce dosing frequency.[4–6] Numerous studies focused on the improvement of the immune performance of PEGylation. The conjugated PEG-hexadecane has a stimulatory adjuvant activity to potentiate a robust humoral and cellular immunity.[7] Incorporation of a small amount of PEG into DOTAP liposomes not only increased the passive lymph nodes targeting of liposomes, but also improved the efficiency of the vaccines.[8] PEGylation of lipopeptide R_4Pam_2Cys facilitated antigen uptake and presentation to T cells and showed improved antigen-specific $CD8^+$ T-cell response.[9] In order to benefit from PEGylation, herein, we use the hydrophobic interaction between lipid to form the nano-carrier, and embellish it with DSPE-PEG_{2000} for a better immunological performance.

For modern adjuvant development, it is normal to combine immunopotentiators with nano-carriers. As a natural source of immunopotentiators, ingredients from herbal medicine have received much attention and made a certain research process. *Rehmannia glutinosa*, a therapeutic Scrophulariaceae herb, has been used for different medical purposes as a traditional Chinese herbal medicine for thousands of years, which was recorded in Chinese medical classics "Shennong's Materia Medica" and was thought as a "top grade" herb. Modern immunological and pharmacological researches have confirmed that *R. glutinosa* polysaccharide (RGP) is the main component of *R. glutinosa* to exert immunological function. According to the literature, RGP significantly upregulated lymphocyte proliferation and its cytokine production.[10] Study of RGP on both mouse bone marrow-derived dendritic cells (BMDCs) and human DCs demonstrated that RGP could effectively stimulate the maturation and activation of the DCs.[10–12] Research on the immune function of mice showed that RGP could increase the indexes of immune organs and ameliorate the swelling of mouse toes, increase the lymphocyte proliferation responses and enhance peritoneal macrophage phagocytosis.[13] It was also found that RGP induced maturation of DCs and activation of T cells and natural killer cells in the mouse in vivo; consequently, the RGP could function as an adjuvant for the treatment of cancer by immunotherapy.[14,15] As a mucosal adjuvant, RGP could effectively increase the number of DCs in the mediastinal lymph node (mLN), the concentration of pro-inflammatory cytokines in the lung and IFN-γ and TNF-α production in the mLN T cells.[16] RGP could also promote the growth rate and strengthen the immune ability in common carp, which suggested that it could be a promising feed additive for *C. carpio* in aquaculture.[17]

Although the confirmed immune profile of RGP, however, when directly applied for clinical, RGP has many disadvantages, such as fast metabolism, short action time, poor targeting effect, large clinical dosage, etc. Therefore, there is an urgent need to optimize the dosage form for a better clinical performance. We nano-sized the immunopotentiator from *R. glutinosa* and formed the PEGylation nano-RGP (pRL). In this study, the preparation conditions of pRL were optimized with response surface methodology (RSM), which is a collection of statistical and mathematical methods used to evaluate complex relationships between multiple parameters and their responses and to identify response optimizing factor combination with a less laborious and reduced number of experimental trials.[18,19]

The immunological function of pRL on macrophage was investigated afterwards. Macrophages, typical phagocytic cells, are derived from peripheral blood monocytes and function as professional antigen-presenting cells. As a phagocytic cell, they could phagocytose pathogens, infected, debris and dead cells. Macrophages play an indispensable role in the immune system with decisive functions in both innate immunity and acquired immunity.

Of note, macrophages can be activated over a range of phenotypes. Two major macrophage sub-populations with different functions include classically activated immune stimulatory phagocytes M1 and alternatively activated anti-inflammatory phagocytic M2 macrophages, which have been reported.[20,21] Functionally, M1 macrophages participate in the removal of pathogens during infection. They are involved in phagocytosis of invasive pathogens and other extracellular particles and produce high levels of proinflammatory cytokines.[22,23]

The aim of our present study was to establish the optimum conditions of preparing the pRL and its optimal lyophilization method. Furthermore, the immunological function on macrophages was compared with that of the nano-RGP without PEGylation, which included the influence of pRL on macrophage proliferation, uptake ability and cytokine section. Also, the endocytosis pathway though which pRL work on macrophages was investigated.

Materials and Methods

Materials

R. glutinosa polysaccharide (with a purity of 98% HPLC, mol. wt: 3.57×10^4, basic structure was purchased from Shanxi Ciyuan Biotechnology Co. Ltd. Soybean phospholipid and DSPE-PEG_{2000} was from Avanti Polar Lipids (Alabaster, AL, USA). Cholesterol was purchased from Sigma Aldrich (St. Louis, MO, USA).

RAW 264.7 cell lines were purchased from American Type Culture Collection (ATCC Manassas, VA). RPMI-1640 (Gibco) was supplemented with benzylpenicillin 100 IU·mL,$^{-1}$ streptomycin 100 IU·mL^{-1} and 10% fetal bovine serum. CCK-8 was purchased from Abcam. Lipopolysaccharide (LPS) was obtained from Sigma-Aldrich. Endocytosis inhibitors, chlorpromazine, cytochalasin D and genistein, were obtained from Sigma Aldrich (St. Louis, MO, USA). Cytokine ELISA reagents, IL-6, IL-12, IL-1β and TNF-α, were purchased from Biolegend (San Diego, CA, USA).

Preparation of pRL

pRL was prepared by thin film hydration method combined with ultra-sonication technique. Lipid and cholesterol were dissolved in chloroform and methanol solution (v/v=1:1). The organic solvent was then removed by rotary evaporation under reduced pressure at room temperature to obtain a thin film on the wall of the round-bottom flask. The vacuum was applied overnight to ensure total removal of trace solvent. The dry film was hydrated with a solution of RGP dissolved in ddH_2O. The dispersion of the lipid was facilitated by mechanical shaking and water bath for 30 mins. The lipid–drug mixture was further rotoevaporated under vacuum for 25 mins. And 2-min homogenization in the ultrasonic cell disintegrator (JY92-II DN, Xinzhi Bio-technology and Science Inc.) was followed to obtain a homogeneous solution. To control the particle diameter, the solution was successively filtered using 0.45-μm and 0.22-μm millipore membrane.

Encapsulation Efficiency and Drug-Loading Rate of pRL

Encapsulation efficiency (EE) was measured by a high-speed centrifuge technique combined with the vitriol-phenol method. One hundred microliters of pRL and 400 μL ddH_2O were added to 1.5-mL EP tube and centrifuged for 30 mins at speed of 13,000 rpm. Twenty-five microliters of the supernatant were used to assay the content of RGP using the vitriol-phenol method, which was referred to as the content of the unencapsulated drug.

The formula to calculate encapsulation efficiency was $EE\% = (1 - C_F/C_T) \times 100\%$, where C_F is the content of the free drug and C_T is the total content of the drug.[24] The formula to calculate the drug-loading rate was $W\% = [(W_T - W_F)/W_P] \times 100\%$, where W_T is the total content of the drug, W_F is the content of the free drug and W_P is the total content of lipid and cholesterol.

Optimization of pRL Preparation Condition

A three-level, three-variable Box–Behnken factorial design (BBD) (Design Expert software, Version 8.0.6, Stat-Ease Inc., Minneapolis, MN) was applied to determine the best combination of preparation parameters for the preparation of pRL. Three extraction variables considered for this research were X_1 (lipid-to-cholesterol molar ratio), X_2 (the addition of DSPE-PEG_{2000} (lipid molar ratio (%)) and X_3 (lipid to drug (w/w)), and the proper range of three variables was determined on the basis of single-factor experiments for the preparation of pRL (Figures S1–S6).

Table 1 lists the whole design consisted of 17 experimental points, five replicates at the center of the design were used to allow for estimation of a pure error sum of squares. The triplicates were performed at all design points in a randomized order. Experimental data were fitted to a quadratic polynomial model and regression

Table 1 Levels and Code of Variables Chosen for Box–Behnken Design

Factors	Code	Levels and Range		
		−1	0	1
A (lipid-to-cholesterol molar ratio)	X_1	4:1	6:1	8:1
B (addition of DSPE-PEG_{2000} (lipid molar ratio (%))	X_2	1%	5%	9%
C (lipid to drug (w/w))	X_3	5:1	10:1	15:1

coefficients were obtained. The non-linear computer generating quadratic model used in the response surface was as follows:

$$Y = C_0 + \sum_{i=1}^{3} C_i X_i + \sum_{i=1}^{3} C_{ii} X_i^2 + \sum_{i=1}^{2} \sum_{j=i+1}^{3} C_{ij} X_i X_j \quad (1)$$

where Y is the measured response associated with each factor level combination; C_0 is an intercept; C_i, C_{ii} and C_{ij} are regression coefficients computed from the observed experimental values of Y; X_i and X_j are the coded levels of independent variables. The terms X_iX_j and X_i^2 represent the interaction and quadratic terms, respectively.

The adequacy of the model was evaluated by ANOVA statistical analysis. The predicted and adjusted R^2 were calculated to evaluate the fitness of the model. The 3D surface graphs were plotted to illustrate the relationship between the responses and the experimental levels of each of the variables. The preferred characteristics of the responses were the higher encapsulation efficiencies for RGP. The point optimization method is employed in order to optimize the level of each variable for maximum response. The combination of different optimized variables, which yield the maximum response, is determined to verify the validity of the model. Subsequently, additional confirmation experiments were subsequently conducted to verify the validity of the statistical experimental design.

Characterization of pRL

The morphology of pRL was observed under transmission electron microscope (Model H-7650, Hitachi, High Technologies Co., Ltd.). Samples were negatively stained with 1% phosphotungstic. The average size of pRL was determined by dynamic light scattering (DLS) at 25 °C at a 90° angle using Zetasizer NanoZS90 instrument (Malvern Instruments, England). Each experiment was repeated three times.

Lyophilisation Method Optimization

After the optimum pRL formulation was obtained, this formulation was used to develop a suitable lyophilized powder by freeze-drying under different conditions.

Various experiments were carried out to determine the best parameters to prepare a pRL lyophilized powder including (1) different kinds of sugar-based cryoprotectant and (2) different ratios of lipid:cryoprotectant.

The formability and redispersibility of the lyophilized pRL were used to evaluate the optimal cryoprotectant. To determine the best lipid:cryoprotectant ratio, the drug encapsulation efficiency after lyophilization was compared with that prior to lyophilization.

Freshly prepared pRL mixed with different cryoprotectants: lactose, sucrose, glucose, xylitol, sorbitol, mannitol, mycose at 1:2 lipid: cryoprotectant mass ratio.

One milliliter of the freshly prepared pRL solution mixed with an aliquot amount of the cryoprotectant stock solutions was filled in 2-mL glass vials. The vials were closed with a rubber stopper and shortly vortexed. And then they were stored in an ultra-low freezer at −80°C overnight. Then, the vials were placed in the drying chamber of the freeze-drier and lyophilized for 24 hrs (Com 6011; Hof Sonderanlagenbau GmbH, Lohra, Germany).

The lyophilization protocol was performed as follows: the samples were placed in the drying chamber precooled to −40°C. The lyophilisation procedure was run for 24 hrs at 8 Pa. After this period, a second drying step was applied at 20°C for 12 hrs under 20 Pa. After the secondary drying, the lyophilized powder was collected and mixed using a sterilized spatula and stored in a desiccator at 4 °C.

Cell Proliferation Experiments

RAW 264.7 cell lines were cultured in DMEM containing 10% fetal bovine serum, 100 IU/mL penicillin and streptomycin in a humidified air with 5% CO_2 at 37 °C. Cells were inoculated in a 96-well plate with a density of 5000 cells/well. After overnight incubation, the medium was replaced with medium (without phenol red) containing different concentrations of pRL, nano-RGP without PEGylation (RL), blank nano-vehicle (BL) and RGP, respectively. LPS was the positive control, while medium alone was set as the negative control. After 40-hr incubation, CCK-8 solution was added to each well and further incubated for 2 hrs. The absorbance values were measured at 450nm.

To determine though which endocytic pathway pRL internalized into RAW264.7 cells, various endocytosis inhibitors were applied. Macrophage cells were planted at a density of 5000 cells/well in the 96-well plates and incubated in complete medium for 24 hrs. The cells were then washed with DHank's twice, followed by preincubating at 37 °C for 1 hr with one of the following endocytosis inhibitors dissolved in serum-free DMEM: chlorpromazine (an endocytotic inhibitor of clathrin-mediated endocytosis), cytochalasin D (an endocytotic inhibitor of macropinocytosis-mediated endocytosis) or genistein (an inhibitor of caveolae-mediated endocytosis).[25] Next, the medium was removed and replaced with complete DMEM containing drugs with different concentrations and different inhibitors for another 40hrs. The cell proliferation was evaluated using CCK-8 method.

Cytokine Assays

RAW264.7 cell was cultured as 2.7. After 40-hr co-culture with different drugs, the cell culture supernatants were collected and assayed for IL-6, IL-12, IL-1β and TNF-α, using ELISA kits from Biolegend, according to manufacturer's instructions with a BioTek Synergy HT Microplate Readers.

Cell Internalization Tests

RAW264.7 cell was cultured as 2.7. Cells were inoculated in 6-well plate with a density of 10^5 cells/well and incubated in complete medium for 24 hrs. After being treated with DiD-labeled drugs for 2–6 hrs, the drug-containing medium was washed. To further determine subcellular distribution, LysoTracker-green (Invitrogen) was used to stain lysosomes after 4 hrs of DiD-labeled pRL incubation. The slides were observed under a confocal laser scanning microscope (Carl Zeiss). To obtain more quantitative and dynamic changes in cellular uptake, flow cytometry (BD FACSCanto™, USA) was also employed to evaluate the cellular uptake of DiD-labeled pRL after incubated for 2 hrs, 4 hrs and 6 hrs.

Statistical Analysis

All values are expressed as the mean ± S.E. Statistical significant differences between groups were determined using one-way or two-way ANOVA following Tukey's or Bonferroni post hoc comparison and Student's *t*-test analysis using GraphPad Prism software (Version 6, San Diego, CA, USA). $P<0.05$ were considered as significant.

Results

Statistical Analysis and Model Fitting

Response surface methodology (RSM) is an effective statistical technique for developing, improving and optimizing complex processes. It allows a more efficient and easier arrangement to solve multivariable data, which are obtained from properly designed experiments to solve multivariable equations simultaneously. A 17-run BBD with three factors and three levels for fitting a second-order response surface was applied to optimize the pRL preparation conditions. The experimental conditions and the EE of pRL according to the factorial design are shown in Table 2. These results also showed that the EE ranged from 80.01% to 94.56%. The maximum EE value (94.56%) was found in conditions of X_1 = 6:1, X_2 = 9% and X_3 = 5:1. The values of the regression coefficients were calculated, and the response variable and test variables were related by the following second-order polynomial equation:

$$Y = 49.67 + 8.09X_1 - 0.39X_2 + 4.57X_3 + 0.32X_1X_2 - 0.39X_1X_3 + 0.02X_2X_3 - 0.53{X_1}^2 - 0.10{X_2}^2 - 0.15{X_3}^2 \quad (2)$$

The statistical significance of the regression model was confirmed using the *F*-test and *P*-value, and the analysis of

Table 2 The Design and Results of Box–Behnken Experiments

No.	X_1: Lipid-to-Cholesterol Molar Ratio	X_2: Doses of DSPE-PEG_{2000}	X_3: Lipid-to-Drug Weight Ratio	Response: EE (%)	
				Predicted EE	Practical EE
1	−1	0	−1	90.86	86.31
2	1	−1	0	82.34	82.41
3	0	−1	−1	89.93	88.57
4	0	1	−1	92.86	94.56
5	−1	1	0	88.03	90.79
6	1	0	1	92.86	80.01
7	0	−1	1	88.05	80.05
8	0	0	0	93.60	91.55
9	−1	−1	0	87.41	90.48
10	0	0	0	92.86	92.02
11	0	1	1	92.86	87.51
12	0	0	0	89.19	92.26
13	−1	0	1	81.21	89.80
14	0	0	0	92.86	94.93
15	0	0	0	92.84	93.51
16	1	1	0	93.39	93.05
17	1	0	−1	78.91	92.23

variance (ANOVA) for the response surface quadratic model is shown in Table 3. The determination coefficient (R^2 = 0.9386), shown using ANOVA of the quadratic regression model, indicated that 93.86% of the variability in the response of EE could be explained using Eq. (2), which indicates that the model was adequate to predict within the range of experimental variables. The *P*-values were used as a tool to confirm the significance of each coefficient. Furthermore, the smaller the *P*-value, the more significant the corresponding coefficient.[26] In this table, the linear coefficients (X_2, X_2, X_3), a quadratic term coefficient (X_1^2 X_3^2) and the interaction coefficient ($X_1 \times X_2$, $X_1 \times X_3$) were significant ($P < 0.05$). The other term coefficients ($X_2 \times X_3$, X_2^2) were not significant ($P>0.05$).

The full model filled Eq. (2) generated three-dimensional and contour plots to predict the relationships between the independent variables and dependent variables.

Optimization of Preparation Condition

The 3-D response surface and 2-D contour plots that are the graphical representations of regression equation obtained from the calculated response surface are indicated in Figure 1.

Table 3 ANOVA for Response Surface Quadratic Model

Source	Sum of Squares	*df*	Mean Square	*F* Value	P Value
Model	342.02	9	38.00	18.24	0.0005 Significant
A	11.72	1	11.72	5.63	0.0495
B	74.37	1	74.37	35.70	0.0006
C	73.81	1	73.81	35.44	0.0006
AB	26.63	1	26.63	12.79	0.0090
AC	61.73	1	61.73	29.63	0.0010
BC	0.54	1	0.54	0.26	0.6252
A^2	19.03	1	19.03	9.14	0.0193
B^2	10.05	1	10.05	4.82	0.0641
C^2	55.81	1	55.81	26.79	0.0013
Residual	14.58	7	2.08		
Lack of fit	7.12	3	2.37	1.27	0.3971 not significant
Pure error	7.46	4	1.87		
Cor total	356.60	16			

Notes: R^2=0.9591, R_{Adj}^2=0.9065, R_{Pred}^2=0.6480.

Three independent response surface plots and their respective contour plots were shown, which made it convenient to analyze the relationship between the responses and experimental levels of each variable and the type of interactions between the two independent variables. The elliptical contours were obtained when there was a perfect interaction between the independent variables.[27,28]

The 3-D response surface and 2-D contour plots in Figure1A show the interaction effect of the lipid-to-cholesterol molar ratio and the addition of DSPE-PEG_{2000} (lipid molar ratio (%)) on EE of pRL. When the lipid-to-cholesterol molar ratio was between 6:1 and 8:1 and the addition amount of DSPE-PEG_{2000} was from 5% to 9%, the optimal EE was obtained.

Figure1B shows the interaction effect of the lipid-to-cholesterol molar ratio and the lipid-to-drug ratio. EE increased when the lipid-to-cholesterol molar ratio changed from 4:1 to 6:1 and then decreased when it was from 6:1 to 8:1. The maximum EE was found to be between 6:1 and 7:1. The change tendency of EE with the lipid-to-drug ratio was similar to that with the lipid-to-cholesterol molar ratio. The maximum EE was achieved when the ratio was around 7:1.

The 3-D response surface plot and contour plot in Figure 1C, which made EE as a function of the addition of DSPE-PEG_{2000} and lipid-to-drug ratio, indicated that the maximum EE was achieved when the addition of DSPE-PEG_{2000} ranged from 7% to 9%, and the lipid-to-drug ratio was around 7:1.

By analyzing these 3-D response surface and their respective contour plots, it is convenient to understand the interactions between two independent variables and their optimum ranges. The optimum preparation conditions for pRL were as follows: lipid-to-cholesterol molar ratio of 8:1, the addition of DSPE-PEG_{2000} of 9% and the lipid-to-drug ration of 5.4:1. Under the above conditions, predicted values were 96.59% from fitted equations, slightly higher than that obtained from plots analysis.

The suitability of the model equation for predicting the optimum response values was tested using the recommended optimum conditions. Four confirmation experiments were conducted under the optimized conditions, and then responses were measured. The mean EE obtained was 95.81±1.58% (n=4). The results indicated that the RSM approach was effective for optimizing the conditions for the preparation of pRL.

Under optimal conditions, the characterization, lyophilisation method and immunological activity pRL were further investigated.

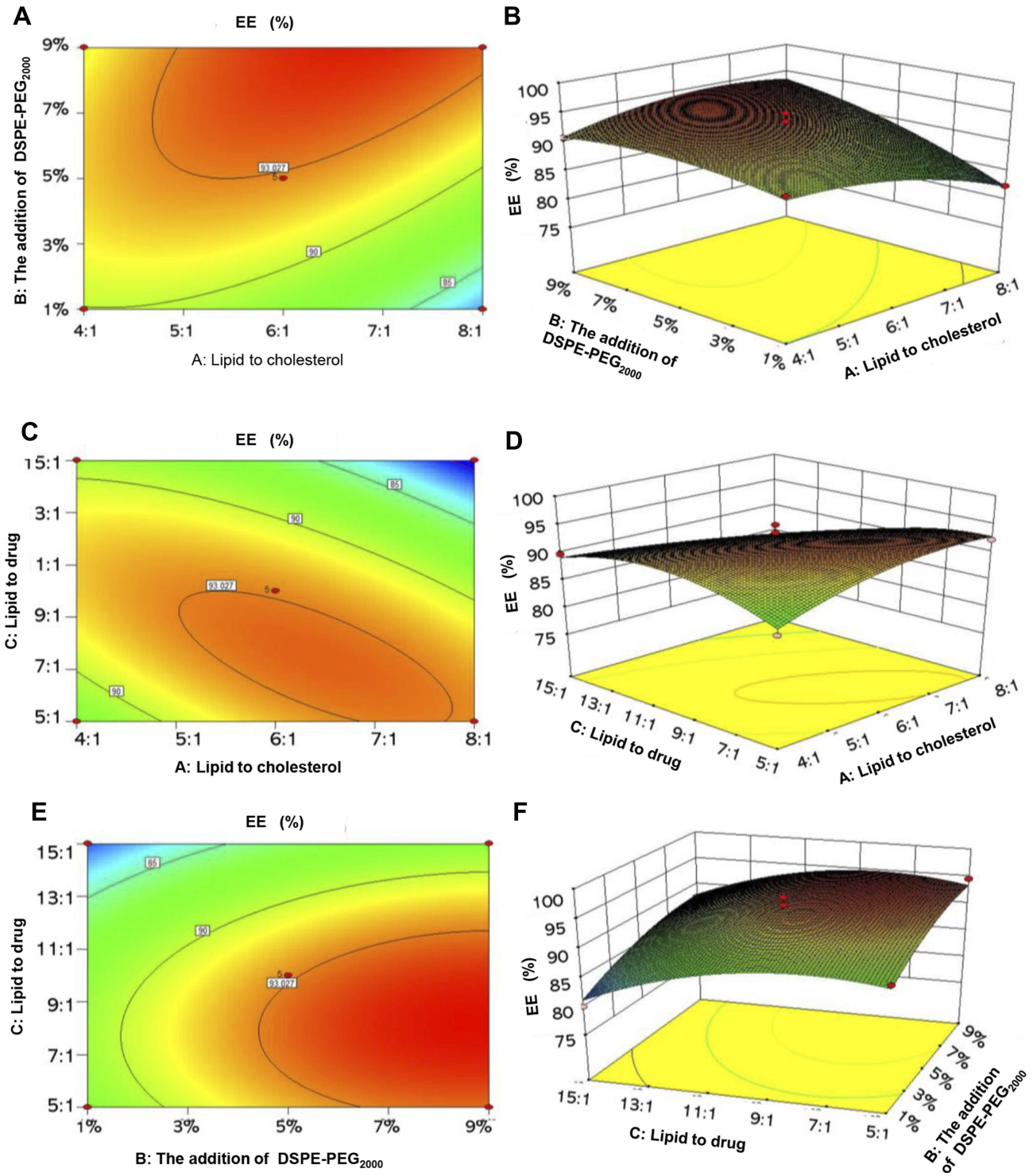

Figure 1 2-D contour plots and 3-D response surface plots showing the effects of various parameters on EE. (**A** and **B**) The effects of X_1 and X_2 on EE. (**C** and **D**) The effects of X_1 and X_3 on EE. (**E** and **F**) The effects of X_2 and X_3 on EE.
Abbreviations: X_1, lipid-to-cholesterol molar ratio; X_2, doses of DSPE-PEG$_{2000}$; X_3, lipid-to-drug weight ratio; EE, encapsulation efficiency.

Characterization of pRL

The macroscopic appearance of pRL formulation showed a homogeneous translucent solution. The color looked like cappuccino due to the drug. The morphology of pRL was observed though H-7650 transmission electron microscope (Figure 2A). The pRL appeared as a spherical particle with

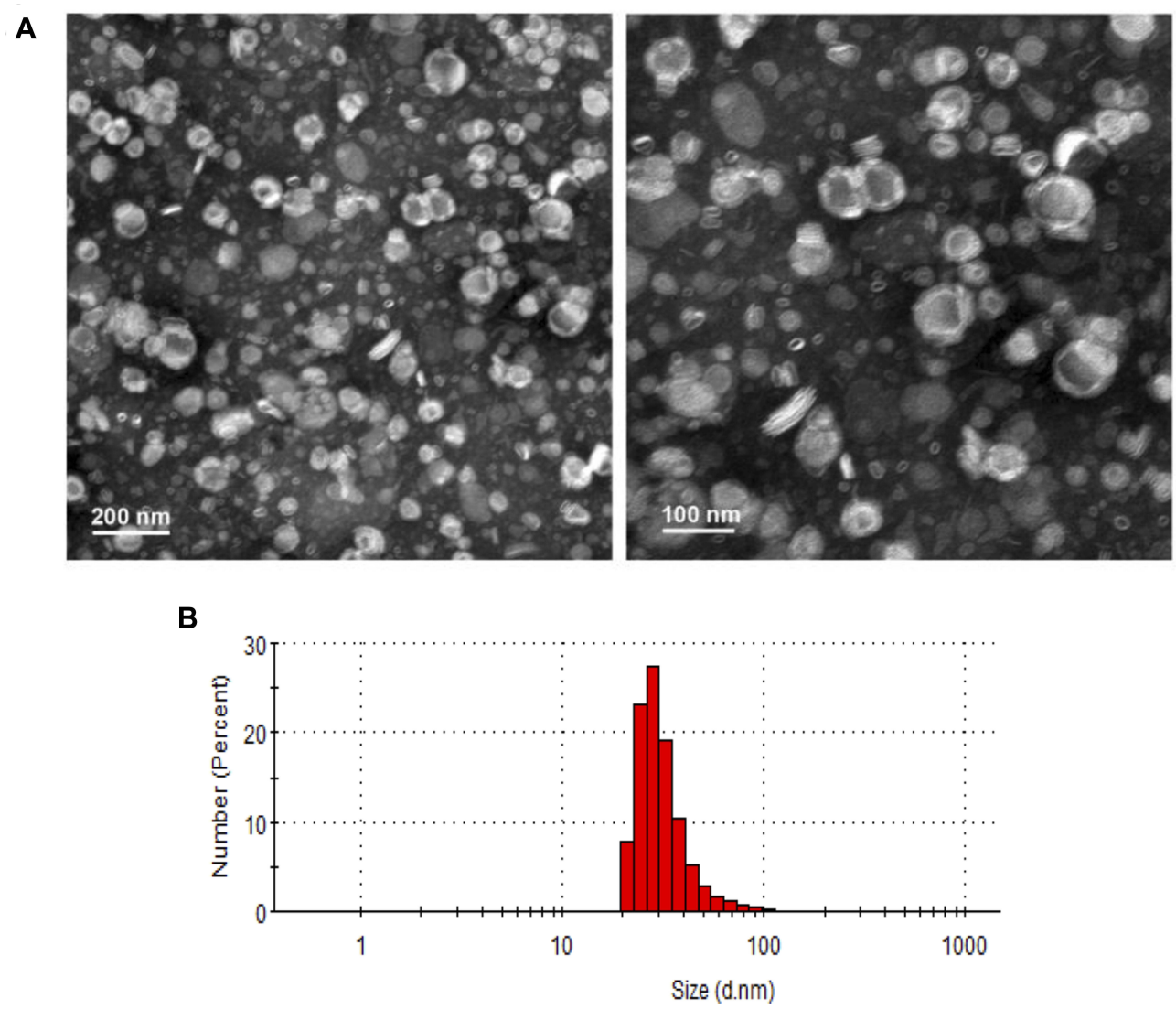

Figure 2 Particle size and morphology of the optimized pRL. (**A**) Morphology of the pRL observed by TEM. (**B**) Particle size of the optimized pRL was measured by DLS.
Abbreviations: pRL, PEGylation nano-RGP; DLS, dynamic light scattering; TEM, transmission electron microscopy.

uniform size. The particle diameter for pRL was 31.98 ± 2.6 nm, and the PDI value was 0.208 (Figure 2B).

Optimization of Lyophilisation Method

After the optimal preparation method for pRL was obtained, the resulting formulation was used to develop a suitable dry powder for long-time storage. Freeze-drying is presently used to achieve long-term stability of nano-particles as drug carrier systems. Under appropriate lyo-protective conditions, nano-carriers should maintain their vesicle size and drugs should remain inside the carrier following freeze-drying and rehydration.

The lyophilisation processes of pRL in the presence of various sugar-based lyoprotectants were compared in order to better enhance the physical stability of our nano-adjuvant. As shown in Table 4, the formability and redispersibility after the lyophilisate reconstitution were evaluated. Lactose, sucrose and mycose were chosen for further dose optimization.

Table 4 The Effects of Different Lyoprotectants on Formability and Redispersibility of the Lyophilized pRL

Cryoprotectant	Formability	Redispersibility
Lactose	+++	++++
Sucrose	++++	++++
Mannitose	++	+
Mycose	++++	++++
Sorbitol	+	++
Glucose	+	+++
Xylitol	+	+++

Abbreviation: pRL, PEGylation nano-RGP.

The lyoprotectant-to-lipid ratio was set at 1:1, 2:1, 3:1 and 4:1. The EE after lyophilisation is listed in Table 5. Also, the drug retention rate was calculated. From the result, it is observed that lactose was the optimal lyoprotectant, and the best sugar-to-lipid ratio was 2:1.

pRL Showed Enhanced Macrophages Proliferation Efficiency

Macrophages are a group of heterogeneous cells of the innate immune system. Their purpose is to maintain tissue homeostasis and act as immune sentinels. They sense structures that contain exogenous or endogenous pathogen-associated molecular patterns and initiate the early promotion of an immune response through the secretion of pro-inflammatory cytokines.[22,29]

To investigate the immunological activity of pRL, the effect on macrophages (RAW 264.7) proliferation was measured by CCK-8 assay. The proliferation of RAW264.7 cells was tested in the presence of pRL, RL, RGP and BL, respectively. All the drugs were in the same drug concentration range (12.5–200 μg/mL) and co-cultured with RAW 264.7 for 40hrs. OD_{450nm} was used as the index for cell proliferation. The results revealed that pRL promoted macrophages proliferation in a dose-dependent manner within 12.5 to 100 μg/mL. Its OD_{450nm} value was significantly higher than that of RL at the concentration between 50 and 100 μg/mL ($P<0.01$) (Figure 3A).

Table 5 Comparision of the EE and the Retention Rate Under Different Lipid-to-Cryoprotectant Ratios

	Lipid: Cryoprotectant	EE After Lyophilization (%)	Retention Rate (%)
Lactose	1:1	91.67±3.02	97.41±2.90
	2:1	92.49±1.15	99.08±1.31
	3:1	86.00±3.82	92.43±4.10
	4:1	88.82±4.16	95.46±4.47
Mycose	1:1	91.26±6.68	95.67±6.53
	2:1	89.19±5.10	95.86±5.49
	3:1	80.87±5.87	86.92±6.31
	4:1	79.73±10.48	85.68±1.26
Sucrose	1:1	59.10±10.82	63.51±1.63
	2:1	60.43±8.34	64.94±8.96
	3:1	73.51±1.17	78.99±1.26
	4:1	70.23±1.19	75.47±1.28

Abbreviation: EE, encapsulation efficiency.

pRL Increased Macrophage Cytokine Production with M1 Polarization Characteristics

Next, we analyzed the pro-inflammatory cytokines induced by pRL, RL, RGP and BL. We incubated pRL, RL, RGP and BL with RAW264.7 cells for 24 hrs and examined the production of IL-6, IL-12, IL-1β and TNF-α by ELISA. LPS was set as positive control and BC was the blank control.

Our results showed that the secretion of IL-6, IL-12, IL-1β and TNF-α stimulated by pRL significantly increased compared with RL at the same concentration (Figure 3B–E). According to the fact that high production levels of pro-inflammatory are the character of M1 phenotype macrophage,[30] the results thus indicated that pRL-stimulated macrophage showed M1 polarization.

pRL Internalized into Macrophage Through Macropinocytosis- and Caveolae-Mediated Endocytosis and Showed Enhanced Cellular Uptake

To understand the mechanisms underlying the enhanced proliferation activity of pRL, we first inspected their uptake in RAW264.7 cells using confocal laser scanning microscopy (Figure 4A). After 2-hr treatment, RL mainly accumulated on the cell membrane, and by contrast, pRL effectively entered RAW264.7 cells and led to substantial intracellular drug accumulation. To show the subcellular location of our nanocarriers, the lysosomes were stained with lysotracker (green fluorescence), and the results showed that the DiD fluorescence was partly colocalized with lysotracker, indicating that pRL was internalized and entered the lysosomes. This enhanced cellular uptake of pRL in RAW264.7 cells was further confirmed by flow cytometry. The pRL effectively internalized and accumulated in a time-dependent manner (Figure 4B and C). And it is significantly higher than that of RL at the same time point. BL hardly showed any cellular uptake during the same period, and it may due to the absence of promotion efficiency of RGP. Collectively, these results suggested that PEGylation and RGP synergistically promoted pRL entery into RAW264.7 cells via a rapid and efficient internalization.

The Endocytic Pathway of pRL Promoted Cell Proliferation

To further uncover the mechanism of pRL entery into RAW264.7, various endocytosis inhibitors were used to

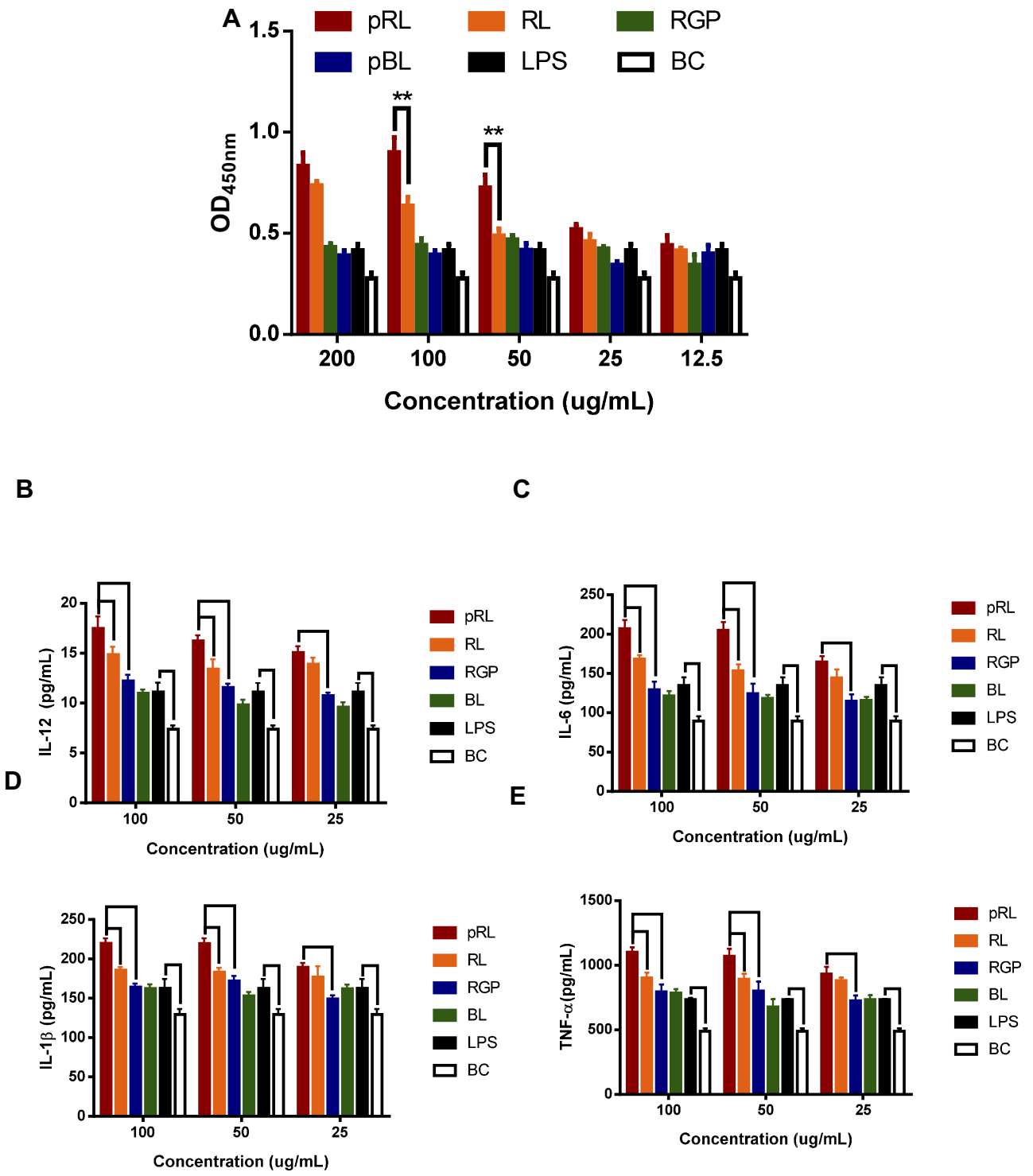

Figure 3 (**A**) Cell viability of RAW264.7 in the stimulation of pRL, RL, BL and RGP at 450nm. LPS was the positive control and the BC was the negative control. (**B-E**) The effects of pRL on the secretion of IL-6, IL-12, IL-1β and TNF-α. (**P<0.01).

Abbreviations: pRL, PEGylation nano-RGP; RL, nano-RGP without PEGylation; BL, blank nano-vehicle; RGP, *Rehmannia glutinosa* polysaccharide; LPS, lipopolysaccharide; BC, blank control.

block the different pathways. Cytochalasin D (an inhibitor of macropinocytosis-dependent endocytosis) and genistein (an inhibitor of caveolae-mediated endocytosis) significantly inhibited the proliferation promotion effect of pRL in a dose-dependent manner, whereas chlorpromazine, an inhibitor of clathrin-mediated endocytosis, did not show any notable

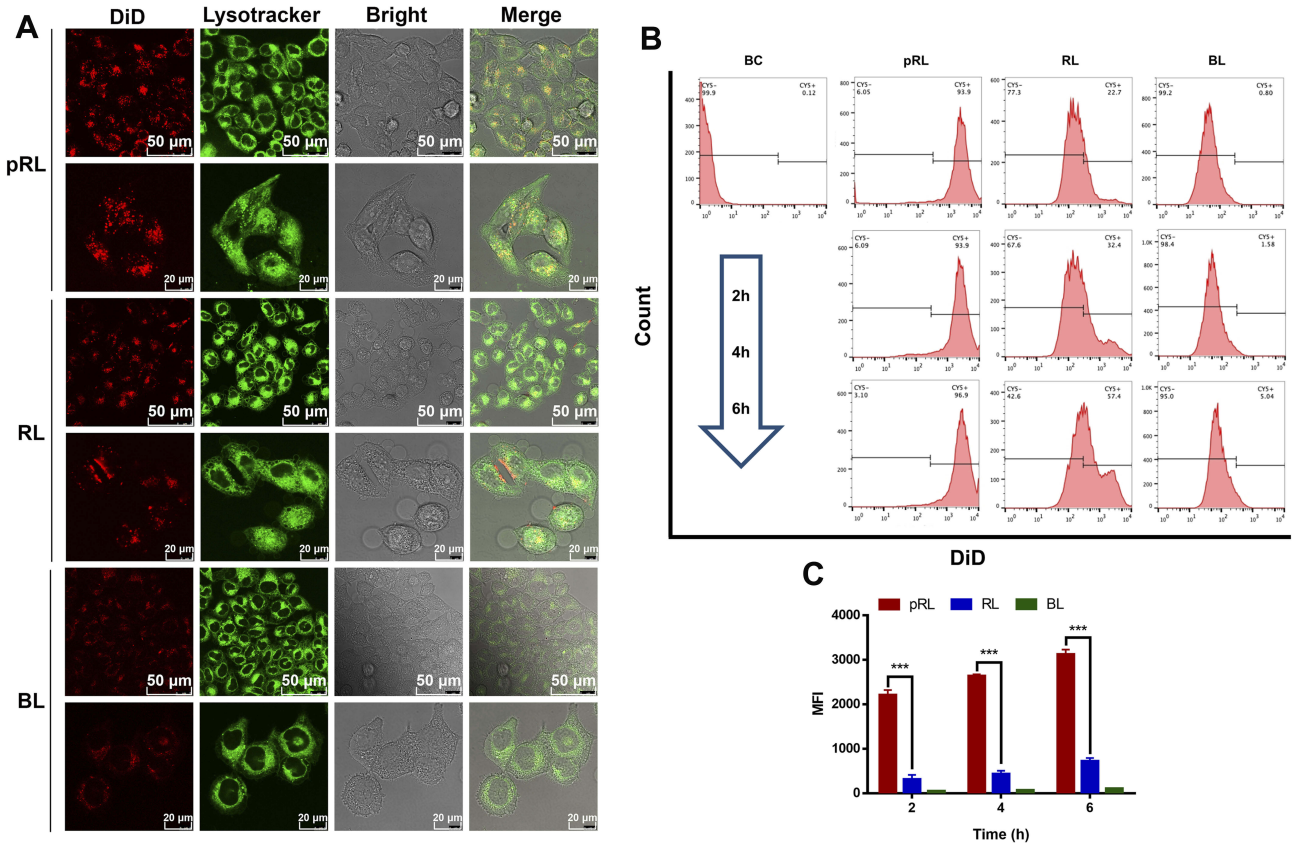

Figure 4 Cellular uptake of RAW264.7 cell lines. (**A**) The intracellular uptake and subcellular distribution of DiD-labeled pRL (50 μg/mL) were investigated after 4hr incubation under the confocal (Green: LysoTracker) (upper line: the scale bar is 50 μm. Lower line: the scale bar is 20 μm). (**B**) The intracellular uptake of DiD-labeled pRL was quantified by flow cytometry. (**C**) The quantification data of the flow cytometry results (***P<0.001).
Abbreviation: pRL, PEGylation nano-RGP.

inhibition on the cellular proliferation promotion effect (Figure 5). All the inhibitors themselves did not show any inhibition effects. The results suggested that macropinocytosis-dependent endocytosis and caveolae-mediated endocytosis were the main uptake mechanisms by which pRL could successfully internalize into RAW264.7 cells, contributing to the effective cell proliferation promotion.

Discussion

Using engineering self-assembled nano-carriers to package antigen and immunopotentiator is a prospective strategy to improve immune activity.[31–33] RGP is the main ingredient of *R. glutinosa* working as an immunopotentiator. In order to achieve sustained release and enhance the delivery performance, the hydrophobic interaction–based assemble of lipid nano-carrier was chosen to protect the active ingredient. Moreover, PEGylation has been employed in this study for the favorable pharmacokinetic consequences.

In our present study, self-assembled PEGylation nano-adjuvant based on *R. glutinosa* polysaccharide was prepared by thin film hydration method combined with ultra-sonication technique. Many factors could influence the drug encapsulation of pRL, such as lipid-to-cholesterol molar ratio, the addition method of DSPE-PEG_{2000}, the addition of DSPE-PEG_{2000}, lipid-to-drug ratio, sonication time, rotavap time and so on. Single-factor experiments have been used to set process variables, but they are time-consuming for obtaining the desired conditions. While, RSM, an effective statistical technique for building empirical models, analyzes the influence and importance of independent variables to one or several dependent variables to improve a process and obtain an optimal response. Multivariate experiments usually reduce the number of assays needed to optimize the process than those obtained by univariate strategies.[34] RSM has been widely applied in optimizing many different process variables.[18,35,36] BBD, one of RSM, only has three levels and needs fewer experiments. It is more efficient and easier to arrange and to

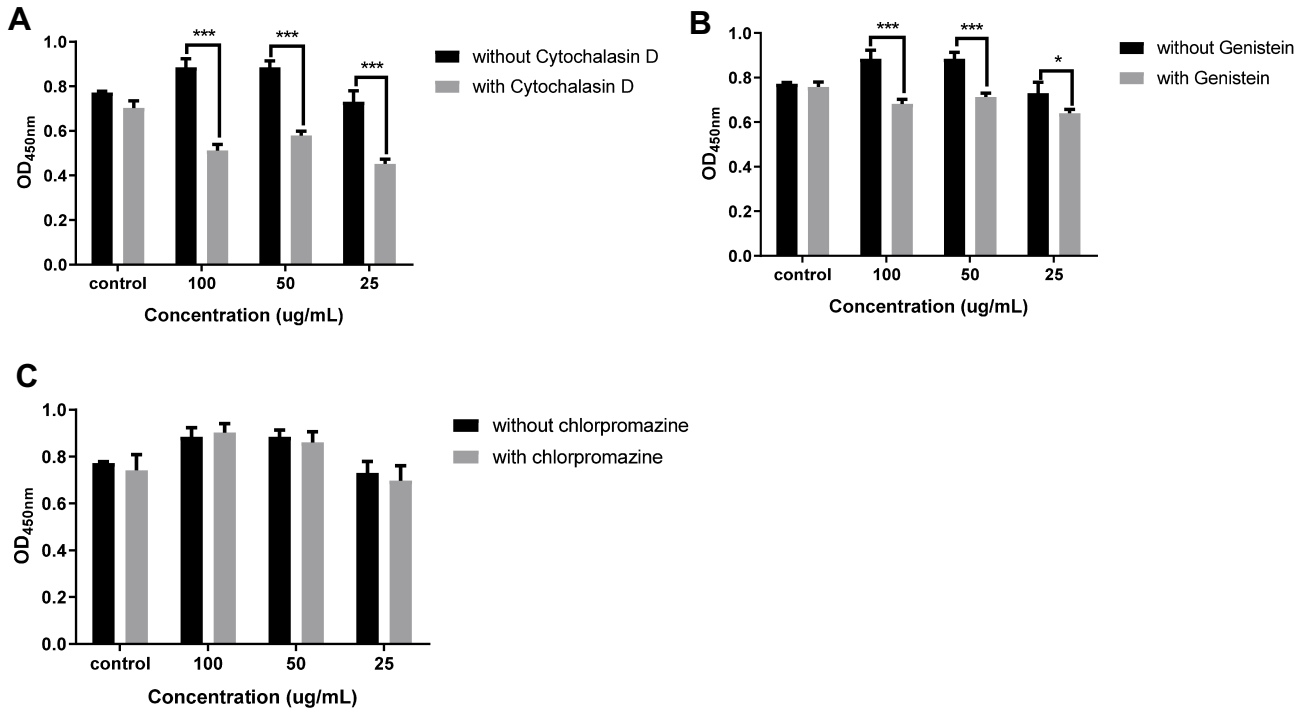

Figure 5 pRL internalized cell via the macropinocytosis- and caveolae-mediated endocytotic pathway. The changes in cell viability by cytochalasin D (**A**), genistein (**B**) and chlorpromazine (**C**) were measured by CCK-8 method (*P<0.05, ***P<0.001).
Abbreviation: pRL, PEGylation nano-RGP.

interpret experiments in comparison with others and widely used by many studies.[19] Herein, it was applied in the optimization of pRL preparation. Establishing the best preparation process is the first and the most important step for developing a novel nano-adjuvant. The size, shape, hydrophobicity and surface modification are the main factors that influence the interactions between nano-adjuvants and the immune system.[37] pRL in the present study appeared as a spherical particle with a compact structure, whose diameter was only 31.98 nm. According to our previous study, the size of RL without PEG was more than 100 nm.[38]

The internalization of nano-carriers in certain cells was highly dependent on size, with the maximum rate of uptake and intracellular concentration occurring within the 25–50 nm size range.[39,40] Our results were consistent with these reports. It showed that after the same incubation time, pRL was particularly evident within lysosomes of macrophages, while RL showed a considerable reduction in cellular uptake. At the same time, BL also decreased cell internalization, which may be due to the lack of synergistic effect of RGP. Due to the size-dependent internalization, the result of cell proliferation further confirmed that the promotion efficacy of pRL on macrophage proliferation was significantly better than that of RL. Moreover, the secretion of cytokines was also significantly increased under the stimulation of pRL compared with RL. The cytokines include IL-6, IL-12, IL-1β and TNF-α, which are one of the characteristic indicators of macrophage M1 polarization. Macrophage polarization is most commonly controlled via exposure to biochemical factors. Recent advances in biomaterial science have identified that biomaterials can be designed to steer macrophage polarity and leveraged to instruct the host's immune response.[41] Our recent study demonstrated that pRL is a potent inducer of the M1 phenotype.

The optimization and character study of pRL laid a good foundation for the following in vitro experiments. In order to illuminate how pRL work on macrophages, three different endocytosis inhibitors were applied on RAW264.7. The inhibitors of macropinocytosis-dependent endocytosis and caveolae-mediated endocytosis showed significant inhibition effect of pRL's proliferation promotion effect on RAW264.7. It can be concluded that pRL entered macrophages and exhibited its immunological function via macropinocytosis-dependent as well as caveolae-mediated endocytosis.

PEGylation made our nano-self-assembled lipid adjuvant more compact and stable. And it also improved the

immunological efficiency of our nano-adjuvant on the macrophage. To obtain long-time storage and achieve long-term stability, lyophilization has been chosen as a promising approach to render the nano-formulation without compromising their size or encapsulation capacity.[42] However, PEG-shell alone was not sufficient to protect our nano-adjuvant upon lyophilization; thus, it was necessary to add cryoprotectants for protecting pRL during dehydration. For those PEGylated nano-self-assembled lipid adjuvants, the compatibility between the lyoprotectants and PEG might influence the protective effect. The protective effect may also be ascribed to the interaction between sugars and phospholipids. According to our results, lactose, sucrose and mycose were suitable lyoprotectants, as it showed better formability and redispersibility of the lyophilized pRL. It might attribute to the fact that lactose, sucrose and mycose are compatible with PEG, whereas other sugars are incompatible with PEG. It is consistent with previous reports by Hinrichs[43] and Yang.[44] Besides the type of lyoprotectants, the lyoprotectant-to-lipid ratio also affects the lyophilization. Our result showed that when the lactose-to-lipid ratio was 2:1, the EE of the drug was 92.49 ± 1.15%, which was the highest compared with others and the drug retention was nearly 100% (99.08 ± 1.31%).

In conclusion, our present study has developed a nano-self-assembled lipid adjuvant based on *R. glutinosa* polysaccharide. The self-assembly offers a unique opportunity to generate simple, well-defined materials with precise control over parameters like shape, size, charge and both relative and absolute loading of drugs. The preparation condition of pRL was optimized in order to obtain a nano-formulation with stable properties and satisfactory immunological function. The optimum preparation condition for pRL was the lipid-to-cholesterol molar ratio of 8:1, the addition of DSPE-PEG_{2000} of 9% and the lipid-to-drug ratio of 5.4:1. Under the above conditions, the experimental EE was 95.81%. Based on the results, lyophilization protectant types on the quality of pRL were evaluated. The optimal lyoprotectant was determined as lactose with a 2:1 sugar-to-lipid ratio.

In this study, a particular emphasis has also been placed on the immunological function of the PEGylation nano-adjuvant on the macrophages. Our results indicated that pRL could significantly promote macrophage proliferation and increase its proinflammatory cytokine production, which made pRL a potent inducer of M1 phenotype polarization. Macrophages stimulated by pRL showed enhanced phagocytosis activation compared with that of the nano-polysaccharide without PEGylation during the same time. From our results, pRL internalized macrophages through macropinocytosis-dependent endocytosis and caveolae-mediated endocytosis, which might contribute to its better immunological performance.

Taken together, our study indicated that the immunological enhancement of RL was significantly enhanced after PEGylation, which made it a better immune adjuvant and provided a theoretical basis for further experiments in vivo.

Acknowledgment

The project was supported by the China Agricultural Research System (No. nycytx-44-3-2), Key Research and Development Plan of Zhejiang Province (No. 2016C02054-10), the Talents Training Program of Zhejiang Academy of Agricultural Sciences (No. 2018R22R08E02), Zhejiang Basic Public Welfare Research Program (Agriculture and Rural Project) (LGN20C180003), and the National Natural Science Foundation (No.31402241).

Disclosure

The authors report no conflicts of interest in this work.

References

1. Vishwakarma A, Bhise NS, Evangelista MB, Rouwkema J, Dokmeci MR, Ghaemmaghami AM. Engineering immunomodulatory biomaterials to tune the inflammatory response. *Trends Biotechnol*. 2016;34(6):435–520. doi:10.1016/j.tibtech.2016.03.009
2. Acar H, Srivastava S, Chung EJ, et al. Self-assembling peptide-based building blocks in medical applications. *Adv Drug Deliver Rev*. 2017;110:65–79. doi:10.1016/j.addr.2016.08.006
3. Eskandari S, Guerin T, Toth IS, Stephenson RJ. Recent advances in self-assembled peptides: implications for targeted drug delivery and vaccine engineering. *Adv Drug Deliver Rev*. 2017;110:169–187. doi:10.1016/j.addr.2016.06.013
4. Vllasaliu D, Fowler R, Stolnik S. PEGylated nanomedicines: recent progress and remaining concerns. *Expert Opin Drug Del*. 2013;11:1–16. doi:10.1517/17425247.2014.866651
5. Veronese FM, Mero A. The impact of PEGylation on biological therapies. *BioDrugs*. 2008;22(5):315–329. doi:10.2165/00063030-200822050-00004
6. Steichen SD, Moore MC, Nicholas AP. A review of current nanoparticle and targeting moieties for the delivery of cancer therapeutics. *Euro J Pharm Sci*. 2013;48:416–427. doi:10.1016/j.ejps.2012.12.006
7. Chang X, Yu W, Ji S, Shen L, Tan A, Hu T. Conjugation of PEG-hexadecane markedly increases the immunogenicity of pneumococcal polysaccharide conjugate vaccine. *Vaccine*. 2017;35(13):1698–1704. doi:10.1016/j.vaccine.2017.02.027
8. Naseri H, Eskandari F, Jaafari M, Khamesipour A, Abbasi A, Badiee A. PEGylation of cationic liposomes encapsulating soluble leishmania antigens reduces the adjuvant efficacy of liposomes in murine model. *Parasite Immunol*. 2017;39(11):e12492. doi:10.1111/pim.12492
9. Sekiya T, Yamagishi J, Gray JHV, et al. PEGylation of a TLR2-agonist-based vaccine delivery system improves antigen trafficking and the magnitude of ensuing antiobody and CD8+ T cell responses. *Biomaterials*. 2017;137:61–72. doi:10.1016/j.biomaterials.2017.05.018
10. Huang Y, Jiang C, Hu Y, et al. Immunoenhancement effect of rehmannia glutinosa polysaccharide on lymphocyte proliferation and dendritic cell. *Carbohydr Polym*. 2013;96:516–521. doi:10.1016/j.carbpol.2013.04.018

11. Zhang Z, Meng Y, Guo Y, et al. Rehmannia glutinosa polysaccharide induces maturation of murine bone marrow derived dendritic cells (BMDCs). *Int J Biol Macromol*. 2013;54:136–143. doi:10.1016/j.ijbiomac.2012.12.005
12. Wang Y, Kwak M, Lee PCW, Jin JO. Rehmannia glutinosa polysaccharide promoted activation of human dendritic cells. *Int. J. Biol. Macromol*. 2018;116:232–238. doi:10.1016/j.ijbiomac.2018.04.144
13. Li H, Hong T, Jiang H, Liu S, Di L. The effects of rehmannia glutinosa polysaccharide on immune function of mice. 2015 7th International Conference on Information Technology in Medicine and Education (ITME). 2015;Huangshan, China. 286–288. doi:10.1109/ITME.2015.63
14. Xu L, Kwak M, Zhang W, Zeng L, Lee PC, Jin JO. Rehmannia glutinosa polysaccharide induces toll-like receptor 4 dependent spleen dendritic cell maturation and anti-cancer immunity. *Oncoimmunol*. 2017;6(7):e1325981. doi:10.1080/2162402X.2017.1325981
15. Xu L, Zhang W, Zeng L, Jin JO. Rehmannia glutinosa polysaccharide induced an anti-cancer effect by activating natural killer cells. *Int J Biol Macromol*. 2017;105:680–685. doi:10.1016/j.ijbiomac.2017.07.090
16. Kwak M, Yu K, Lee PC, Jin JO. Rehmannia glutinosa polysaccharide functions as a mucosal adjuvant to induce dendritic cell activation in mediastinal lymph node. *Int J Biol Macromol*. 2018;120:1618–1623. doi:10.1016/j.ijbiomac.2018.09.187
17. Wang JL, Meng X, Lu RH, et al. Effects of Rehmannia glutinosa on growth performance, immunological parameters and disease resistance to Aeromonas hydrophila in common carp (Cyprinus carpio L.). *Aquaculture*. 2015;435(1):293–300. doi:10.1016/j.aquaculture.2014.10.004
18. Majdia H, Esfahania JA, Mohebbi M. Optimization of convective drying by response surface methodology. *Comput Electron Agr*. 2019;156:574–584. doi:10.1016/j.compag.2018.12.021
19. Niizawa I, Espinaco BY, Zorrilla SE, Sihufe GA. Natural astaxanthin encapsulation: use of response surface methodology for the design of alginate beads. *Int J Biol Macromol*. 2019;121:601–608. doi:10.1016/j.ijbiomac.2018.10.044
20. Kim B, Pang HB, Kang J, Park JH, Ruoslahti E, Sailor MJ. Immunogene therapy with fusogenic nanoparticles modulates macrophage response to Staphylococcus aureus. *Nat Commun*. 2018;9:1969. doi:10.1038/s41467-018-04390-7
21. Hatami E, Mu Y, Shields DN, et al. Mannose-decorated hybrid nanoparticles for enhanced macrophage targeting. *BB Reports*. 2019;17:197–207. doi:10.1016/j.bbrep.2019.01.007
22. Rodriguez AE, Ducker GS, Billingham LK, et al. Serine metabolism supports macrophage IL-1β production. *Cell Metab*. 2019;29(4):1003–1011. doi:10.1016/j.cmet.2019.01.014
23. Shapouri-Moghaddam A, Mohammadian S, Vazini H, et al. Macrophage plasticity, polarization, and function in health and disease. *J Cell Physiol*. 2018;233:6425–6440. doi:10.1002/jcp.26429
24. Liu T, Zhu W, Han C, et al. Preparation of glycyrrhetinic acid liposomes using lyophilization monophase solution method: preformulation, optimization, and in vitro evaluation. *Nanoscale Res Lett*. 2018;13:324. doi:10.1186/s11671-018-2737-5
25. Wei T, Chen C, Liu J, et al. Anticancer drug nanomicelles formed by self-assembling amphiphilic dendrimer to combat cancer drug resistance. *P Natl Acad Sci USA*. 2015;112(10):2978–2983. doi:10.1073/pnas.1418494112
26. Liu Z, Ma X, Deng B, et al. Development of liposomal Ganoderma lucidum polysaccharide: formulation optimization and evaluation of its immunological activity. *Carbohydr Polym*. 2015;117(6):510–517. doi:10.1016/j.carbpol.2014.09.093
27. Chen J, Liu D, Shi B, Wang H, Cheng Y, Zhang W. Optimization of hydrolysis conditions for the production of glucomanno-oligosaccharides from konjac using-mannanase by response surface methodology. *Carbohydr Polym*. 2013;93(1):81–88. doi:10.1016/j.carbpol.2012.05.037
28. Yin X, You Q, Jiang Z. Optimization of enzyme assisted extraction of polysaccharides from Tricholoma matsutake by response surface methodology. *Carbohydr Polym*. 2011;86(3):1358–1364. doi:10.1016/j.carbpol.2011.06.053
29. Weigert A, Knethen A, Fuhrmann D, Dehne N, Brune B. Redox-signals and macrophage biology. *Mol Aspects Med*. 2018;63:70–87. doi:10.1016/j.mam.2018.01.003
30. Sridharan R, Cameron AR, Kelly DJ, Kearney CJ, O'Brien FJ. Biomaterial based modulation of macrophage polarization: a review and suggested design principles. *Mater Today*. 2015;18:313–325. doi:10.1016/j.mattod.2015.01.019
31. Titta AD, Ballester M, Julier Z, et al. Nanoparticle conjugation of CpG enhances adjuvancy for cellular immunity and memory recall at low dose. *P Natl Acad Sci USA*. 2013;110:19902–19907. doi:10.1073/pnas.1313152110
32. Koker SD, Cui J, Vanparijs N, et al. Engineering polymer hydrogel nanoparticles for lymph nodetargeted delivery. *Angew Chem Int Edit*. 2016;55(4):1334–1339. doi:10.1002/anie.201508626
33. Zeng Q, Jiang H, Wang T, Zhang Z, Gong T, Sun X. Cationic micelle delivery of Trp2 peptide for efficient lymphatic draining and enhanced cytotoxic T-lymphocyte responses. *J Control Release*. 2015;200:1–12. doi:10.1016/j.jconrel.2014.12.024
34. Myers RH, Montgomery DC, Anderson-Cook CM. *Response Surface Methodology: Process and Product Optimization Using Designed Experiments*. Hoboken, New Jersey: John Wiley & Sons, Inc.; 2016.
35. Zhong K, Wang Q. Optimization of ultrasonic extraction of polysaccharides from dried longan pulp using response surface methodology. *Carbohydr Polym*. 2010;80:19–25. doi:10.1016/j.carbpol.2009.10.066
36. Mourabet M, El Rhilassi A, El Boujaady H, Bennani-Ziatni M, Taitai A. Use of response surface methodology for optimization of fluoride adsorption in an aqueous solution by brushite. *Arab J Chem*. 2017;10:S3292–S3302. doi:10.1016/j.arabjc.2013.12.028
37. Liu Y, Hardie J, Zhang X, Rotello VM. Effects of engineered nanoparticles on the innate immune system. *Semin Immunol*. 2017;34:25–32. doi:10.1016/j.smim.2017.09.011
38. Huang Y, Wu C, Liu Z, et al. Optimization on preparation conditions of Rehmannia glutinosa polysaccharide liposome and its immunological activity. *Carbohydr Polym*. 2014;104:118–126. doi:10.1016/j.carbpol.2014.01.022
39. Jiang W, Kim BY, Rutka JT, Chan WC. Nanoparticle-mediated cellular response is size-dependent. *Nat Nanotechnol*. 2008;3:145–150. doi:10.1038/nnano.2008.30
40. Albanese A, Tang PS, Chan WC. The effect of nanoparticle size, shape, and surface chemistry on biological systems. *Annu Rev Biomed Eng*. 2012;14:1–16. doi:10.1146/annurev-bioeng-071811-150124
41. Cha BH, Shin SR, Leijten J, et al. Integrin-mediated interactions control macrophage polarization in 3D hydrogels. *Adv Healthc Mater*. 2017;6:1700289. doi:10.1002/adhm.201700289
42. Parise A, Milelli A, Tumiatti V, Minarini A, Neviani P, Zuccari G. Preparation, characterization and in vitro evaluation of sterically stabilized liposome containing a naphthalenediimide derivative as anticancer agent. *Drug Deliv*. 2015;22:590–597. doi:10.3109/10717544.2013.861042
43. Hinrichs WL, Sanders NN, Smedt DSC, Demeester J, Frijlink HW. Inulin is a promising cryo- and lyoprotectant for PEGylated lipoplexes. *J Control Release*. 2005;103:465–479. doi:10.1016/j.jconrel.2004.12.011
44. Yang T, Cui FD, Choi MK, et al. Enhanced solubility and stability of PEGylated liposomal paclitaxel: in vitro and in vivo evaluation. *Int J Pharmaceut*. 2007;338:317–326. doi:10.1016/j.ijpharm.2007.02.011